Mobile X-ray Tomography System with Intelligent Sensing for 3D Chest Imaging

Yang Zhao[a], J. Eric Tkaczyk[a], Alex Chen[b], Bernhard Claus[a], Katelyn Nye[c], Gireesha Rao[c]

[a]GE Research, One Research Circle, Niskayuna, NY, USA 12309; [b]Dept. of Mathematics, California State University, Dominguez Hills, 1000 E. Victoria Street Carson, CA, USA 90747; [c]GE Healthcare, 3000 N Grandview Blvd, Waukesha, WI 53188

ABSTRACT

Tomography in the mobile setting has the potential to improve diagnostic outcomes by enabling 3D imaging at the patient's bedside. Using component testing and system simulations, we demonstrate the potential for limited angle X-ray tomography on a mobile X-ray system. To enable mobile features such as low weight, size and power of system components, we have developed detector and patient anatomy tracking algorithms for accurately and automatically registering system geometry to patient anatomy during acquisition of individual projective-views along a tube-motion trajectory. We evaluate the effects of acquisition parameters and registration inaccuracy on image quality of reconstructed chest images using realistic X-ray simulation of an anthropomorphic numerical phantom of the thorax.

Keywords: X-ray tomosynthesis, 3D imaging, intelligent system, mobile sensing

1. INTRODUCTION

Recent study shows that tomosynthesis can improve diagnostic value of chest X-ray in a mobile setting [1]. However, for current clinical systems offering limited-angle 3D imaging, such as fixed-room X-ray system or c-arm interventional X-ray system, precise and robust geometric registration is ensured by heavy, rigid mechanical supports of the tube-head and detector where alignment is achieved by pre-scan system calibration. Prescribed motion along tomographic trajectories in such systems is actuated by relatively massive and heavy motor drives. The mechanical-registration means of these current 3D imaging systems is not conducive to fast, flexible and convenient positioning requirements of a mobile X-ray system that needs to be transported to and then operated at the patient's bedside.

In this paper, we propose to employ an intelligent visual and inertial sensing mechanism [2] for geometric registration that allows less constrained and less powerful motion-control components. In particular, we consider a mobile acquisition workflow involving placement of a portable detector that is manually positioned between the patient's back and bed-mattress and having no fixed mechanical connection to the system, floors or walls, as is required for current 3D imaging systems. Clinical technicians and nurses who operate mobile X-ray systems today are familiar with the placement of the X-ray detector in this configuration but are imperfect regarding whether the entire area of a large organ, such as the lung, will be captured in the image. Inaccurate positioning is a leading cause of retakes [3]. Thus, we propose to use visual and inertial sensors to track the portable detector and patient anatomy, which can assist the operator in positioning the detector relative to the patient and potentially lead to lower retakes. We also perform X-ray simulations to investigate the impact of mobile system parameters and positioning inaccuracy on image quality of reconstructed tomosynthesis images.

2. METHODS

In a mobile X-ray system used for chest imaging of a recumbent patient, it is anticipated that the motorized arm holding the tube head is initially positioned at a fixed distance away from the patient with the collimator opening adjusted to illuminate the height and width of the patient's chest. As shown in Figure 1, a detector is placed manually between the bed and patient's back and remains stationary during the tomographic scan. Existing capabilities for on-detector data storage will provide adequate number of views to be acquired that allow for high quality tomographic reconstructions. However, inaccuracies of the detector tracking will cause image artifacts and blur. Additional sources of image blur include focal spot width, detector pixel size, tube motion during expose period. For accurate detector positioning, optical markers are attached to the part of the detector's housing that extends beyond the patient's side and remain visible for the purpose of detector tracking exclusively during some periods of the positioning workflow. For situations when markers become partly

or fully occluded, measurements from an inertial measurement unit (IMU) sensor are combined with visual images to track the position and orientation of the detector. That is, geometric registration in a mobile X-ray system can be achieved by leveraging inertial sensors and RGB camera views with optical and X-ray opaque markers. System-level physics simulation and laboratory prototyping and testing are used to quantify the precision of geometric registration and the image quality metrics of reconstructed 3D image slices. To investigate the effect of tracking accuracy on image quality, simulations with system physics model are run for different proposed system parameters, e.g., sweep angle, projection density. The ability to separately resolve anatomical structures at different depths through the thorax is analyzed with simulation results. For example, of clinical interest is the ability to distinguish subtle lung nodules that are superimposed with rib-structures across the height-above-detector dimension.
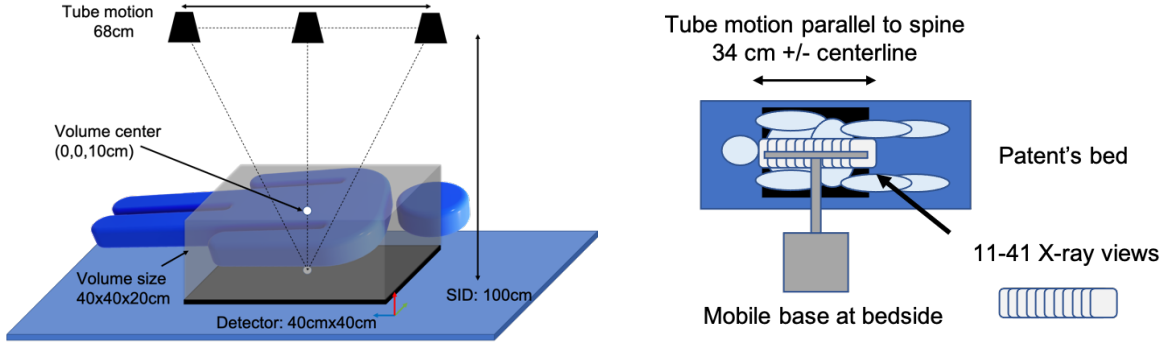

Figure 1 Geometry of mobile X-ray simulation and tomosynthesis reconstruction (left) and mobile system design (right)

2.1 X-ray detector tracking and patient anatomy tracking

To achieve precise geometric registration, we propose to use a visual inertial sensor fusion approach for X-ray detector tracking and use computer vision-based algorithm for patient body part detection and anatomy tracking. The registration capabilities are developed for dual purposes. One is to ensure image quality by providing accurate angle-data entering the tomographic reconstruction. Another purpose is to provide real-time feedback that can ease the acquisition workflow involving portable detector placement and anatomical positioning. Feedback can ensure that the acquisition data can be used to present reconstructed image slices over the full lung organ.

For estimating the orientation and position of a planar object, such as the X-ray detector, the classical perspective-n-point (PnP) algorithm can be used [8]. However, a limitation of the PnP algorithm is that its performance significantly depends on the robust detection of keypoints. Occlusion, illumination changes, and errors in correspondences can all lead to failure of keypoint detection. That is, when certain markers are not visible, e.g., blocked by patient's body, PnP algorithm does not work anymore. Thus, we have developed an algorithm called inertial perspective-n-point (IPNP) algorithm [6] to track the 6-DOF of the detector. The IPNP algorithm improves the robustness of position and orientation estimation by combining IMU measurements with keypoints from RGB camera images, and it reduces the number of keypoints that need to be detected by the camera. While the PnP algorithm needs at least four keypoints for estimating the pose of a planar object, the IPNP algorithm only requires two keypoints visible to the camera.

Patient anatomy and its position within the imaging geometry context was inferred by pose estimation from camera views. Since there may be multiple persons, patient and detector operator, in the camera view, we apply the state-of-the-art part affinity fields (PAFs) algorithm [7] to learn to associate body parts, i.e., keypoints, with each person in the image. Then we can perform anatomy registration based on the detected keypoints. By registering the detected keypoints to keypoints on a canonical subject, an estimated position of the lung X-ray can be computed.

2.2 Anatomy and mobile X-ray simulation

In our anatomy simulation, we use the virtual family Duke anatomical model [5] to create our chest model with four issues, i.e., lung, spine, ribs, and soft tissues. We also create artificial nodules, spheres with radii of 0.5cm and 0.2cm. Then, we add Poisson noise to the projections in order to better represent the image quality achieved by a physical system. The number of photons N that arrive at the detector can be modeled as:

$$N = P(N_0 e^{-L}),$$

where P represents the Poisson distribution, $L = \int_{l_s}^{l_d} \mu dl$ is the linear integration along ray l from source to detector, N_0 is the number of photons emitting from the source at a given electronvolt for chest scan, and μ is the X-ray mass attenuation coefficient, in which we use coefficients from NIST [4] to represent attenuations for different materials and tissues.

For our mobile X-ray system simulation, we assume the detector has a standard size of 40cm by 40cm with in-slice resolution of 0.02 cm. As shown in Figure 1, the X-ray tube moves parallel to spine, with a sweep angle of ±20 degrees, a source to image distance (SID) of 100 cm, and a source to object distance (SOD) of 90 cm. For X-ray tomography reconstruction, we use filtered back projection to reconstruct data into slices with a slice depth resolution of 0.1cm. The volume matrix size is set to be 40cm by 40cm by 20cm, with the central plane 10cm above the detector plane, and thus we have 200 tomosynthesis slices. For the effect of tomography acquisition parameters on image quality, previous study [9] investigated system parameters including sweep angle, number of projections, dose, etc. In a mobile setting, detector position tracking and tube motion can cause geometric registration error, which also affects image quality. To study the effect of the positioning error, we model the relative detector to tube positioning error as Gaussian noise. Since the detector is stationary while the tube moves, the detector positioning error from our tracking system is fixed, and the variation from tube motion can be modeled as a Gaussian distribution with its mean and standard deviation parameters.

3. RESULTS

3.1 Visual-Inertial Registration

3D registration for the purpose of a tomographic scan includes the three position and three rotational degrees of freedom (DOF) for the stationary detector relative to each X-ray source focal spot. A camera view of four markers in a plane with known configuration is sufficient information to reconstruct the 6-DOF, as shown in Figure 2 (center). The IMU is accurate only in the three angular DOF, but robustness to optical occlusion is achieved by algorithmically combining the inertial sensor and camera data [6]. The advantage of the visual inertial sensor fusion IPNP algorithm is that it can track 6-DOF even when certain optical markers are occluded by an object, as shown in Figure 2 (right). Note that only two markers are visible in the camera's view in Figure 2 (right), compared to the four markers case in Figure 2 (center). Due to different process chains for the optical and inertial positioning, analysis finds a 100-millisecond lag between the IMU and camera data, as shown in Figure 2 (left). With rapid motion of the detector, this delay can be compensated by shifting the time axis appropriately.

Figure 2 An IMU mounted to the detector measures three rotation angles that closely follow the camera-based angle except for a lag (left) due to acquisition and wireless communication delays; tracking of the detector 6-DOF position and rotation with the camera combined with 3-DOF rotation from the IMU can accommodate partial visual occlusion (right) of the detector in the camera's field of view.

3.2 Patient Anatomy Tracking

Figure 3 shows examples of our anatomy tracking application used to assist the operator in aligning the system. It consists of an enhanced reality video consisting of the (estimated) lung-organ and detector's active area superimposed onto the live patient image. A Red/Green border to the detector area indicates whether the entire lung will be captured in the acquired X-ray image. In this way the positioning of the patient can be made more accurate. The same system can be used to automatically adjust the collimator blades during the tomographic scan so as to illuminate only the detector's active area.
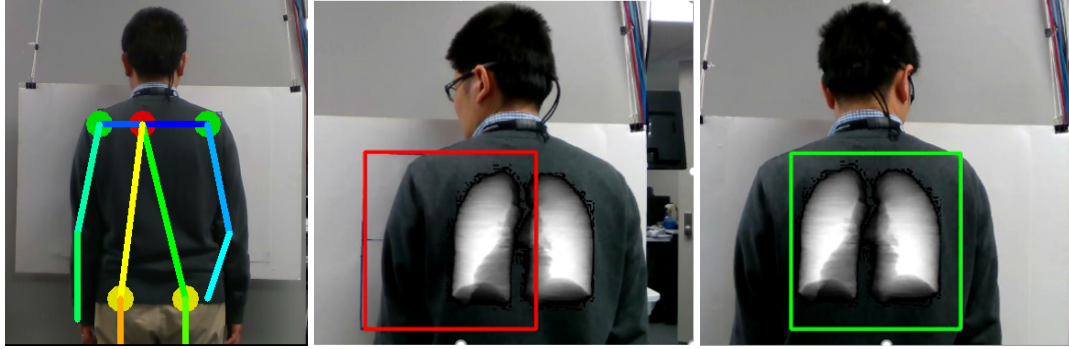
Figure 3 Real time pose estimation in the live video stream (left) identifies anatomical markers to which organ size and positioning can be registered to the detector active area. A red/green boundary box (center/right) indicates whether the entire lung will appear in the acquired X-ray.

3.3 Tomographic IQ analysis through system simulation

Through simulation of a tomographic chest scan, we consider tomographic system design and workflow parameters that influence the ability to separate anatomical structures associated with lung pathology such as nodules, consolidations and subtle pneumothorax which might otherwise be superimposed with normal lung parenchyma and ribs in standard 2D projection radiography.

We first investigate the impact on image quality from constrains in a mobile X-ray setting. Due to physical constraints at the bedside of the patient and cost/weight factors, the travel distance of the tube head during the tomographic scan may be reduced relative to that typically used in the fixed-room system. Figure 4 demonstrates the impact of reducing the sweep angle from 40 to 10 degrees with a fixed 1-degree angular space. For the 10 degrees scan, a 1cm diameter, spherical lung nodule is not easily seen among the crossing rib-structures. In this case slices at different heights look somewhat similar. However, the more 3D-character of a 40 degrees scan can discriminate the nodule and rib-structure due to separation in height position within the lung. The contrast metric that we defined in Section 2.2 is 0.696 and 0.693 for 11 and 41 views, respectively. The background dynamic metric is 6.751 and 5.001 for 11 and 41 views, respectively. Then the image quality metric is 0.103 and 0.139 for these two cases. As shown in Figure 4, the image from 41 views indeed shows the nodule more clearly, while the nodule is not easily identifiable from ribs from fewer views. From Figure 4, we also see that the nodule becomes blurry when the slice is 2cm away from the central plane. In addition, we also investigate the effect of the projection density, i.e., angular space, on the image quality. Fixing the sweep angle as 40 degrees, we increase the angular interval from 1 degree to 2 and 4 degrees. That is, we have 41, 21 and 11 views for a fixed sweep angle of -20 degrees to 20 degrees. From Figure 5, we see that the image quality from 11 views is slightly lower than the other two images, but the nodule on the left lung is visible in all three images. While the nodule cannot be visibly identified from the projective 2D X-ray image, as shown in Figure 5 (left).

Tomographic scanning in the fixed-room system benefits from calibrated, mechanical alignment. An increased degree of geometric imprecision and inaccuracy may be expected for the visual-inertial tracking mechanisms. In addition, patient motion during the scan may be more likely for the critically ill patient and occur as rigid or non-rigid body movement, e.g., breathing. Thus, we further investigate the impact of geometric inaccuracy of focal spot positioning with our simulation. In the simulation, we model the positioning error as Gaussian noise, and Figure 6 illustrates the impact of various registration inaccuracy cases, i.e., Gaussian noises, for a reconstruction of 21 focal spot positions and 20 degrees angular range. If no geometric registration error in the simulation, we can see the nodule clearly in Figure 6 (far left). If we introduce 2cm bias, e.g., a constant detector tracking error, to the focal spot 3D position, the tomography reconstruction is shown in the left image of Figure 6. If we include variation in relative tube-detector positioning, e.g., the Gaussian distribution has a standard deviation of 1cm, the reconstruction result is shown in the right image of Figure 6. If we increase the standard deviation to 2cm, the image is further blurred, as shown in the image on far right. Since the nodule from the right image is clearer than those from the left image, this initial sensitivity study implies that the impact on image quality from position precision, i.e., positioning variation, may be greater than that from a constant positioning bias. The impact is loss of resolution and potentially artifacts in slice images. For these initial simulations, it is assumed that the anatomical plane parallel to the spine and sternum are aligned to the detector plane as is typically achieved in a standing, wall-stand

exam. Additional simulations will consider the image quality impact of anatomy offsets, rotation and tilting that might occur due to non-ideal positioning of the bed-ridden patient.
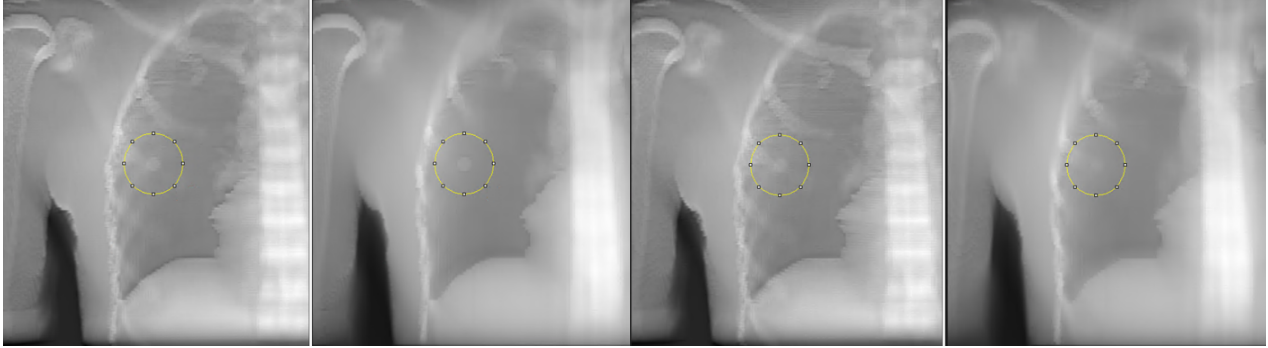

Figure 4 Tomographic slice images at the center plane of a subtle lung nodule (left two) and 2cm anterior (right two) are shown for wide (40 degrees) and narrow (10 degrees) tomographic scan angles. Increased tomographic angle yields better anatomical height discrimination.
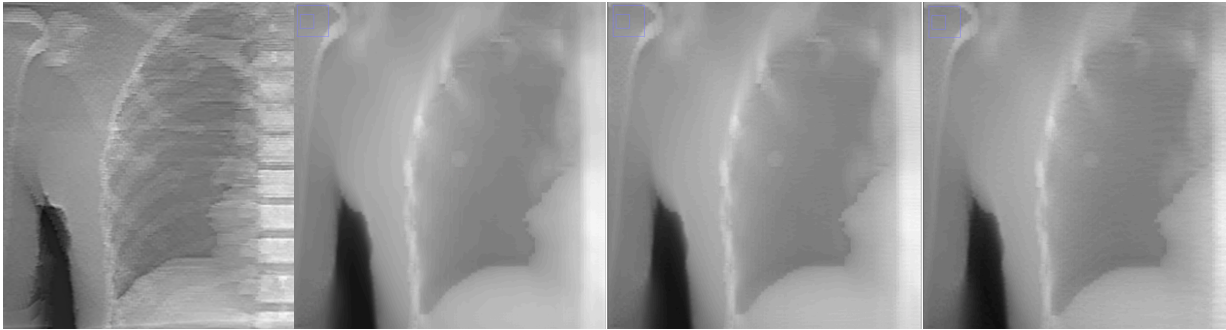

Figure 5 Images from 2D projective X-ray (far left) and 3D tomosynthesis with different numbers of views and different angle ranges, 11 views and 40 degrees angle range (left), 21 views and 40 degrees range (right), and 41 views and 40 degrees range (far right).
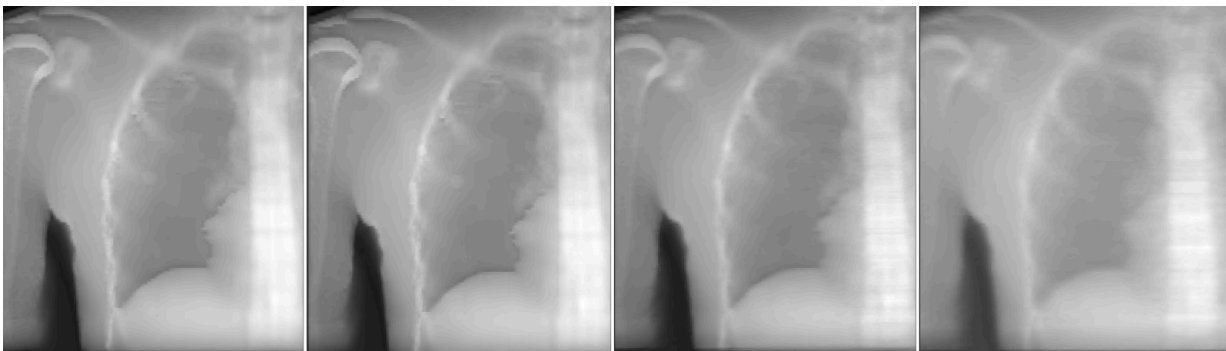

Figure 6 Increased image blurring in slice images occurs as the precision of geometric resolution degrades: exact focal sport position (far left), 2cm bias (left), 1cm standard deviation (right), 2cm standard deviation (far right).

Finally, we investigate image quality (IQ) with our simulation to obtain insights for system design purpose. For determining the sweep angle and projection density parameters, we run simulations for five parameter combinations: 11 views over a sweep angle of 10 degrees, 11 views over 40 degrees, 21 views over 20 degrees, 21 views over 40 degrees, and 41 views over 40 degrees. Then we use contrast-to-noise ratio (CNR) to measure image quality. That is, we measure the contrast by using the absolute difference in the mean intensity of an area of interest, i.e., nodule, with and without the nodule. Noise is measured by the standard deviation of intensities inside a larger circle without the nodule in the image, as shown by the yellow circle in Figure 4. The CNRs for five parameter combinations are shown in Figure 7 (left). As

expected, the simulation result from 41 views over 40 degrees has the highest CNR value, while the lowest CNR is from the 11 views and 10 degrees case, for both small-sized (0.2cm radius) and medium-sized (0.5cm radius) nodules. More interestingly, we find that the CNR from 11 views and 40 degrees is slightly higher than that from 20 views and 20 degrees. That is, a mobile X-ray tomographic system can benefit more from having a larger sweep angle than a larger projection density. For the impact of the focal spot positioning error, Figure 7 (right) shows the CNRs for various standard deviations that we used in simulating the relative tube to detector position error. The CNRs for small and medium sized nodules both decrease significantly when the positioning standard deviation is greater than 0.4cm. This sensitivity study clearly shows the importance of the tube motion control and detector tracking accuracy to the image quality of a mobile X-ray system.
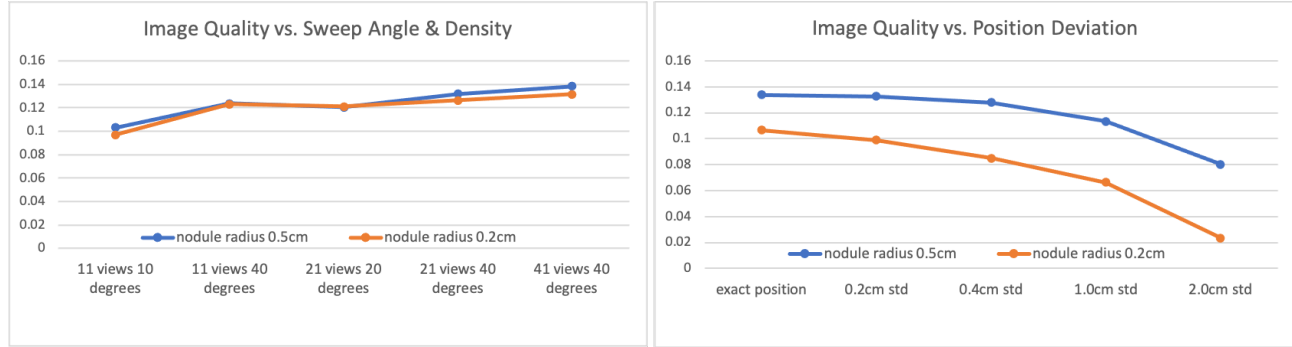

Figure 7 CNRs for various angular range and space combinations (left) and positioning errors (right).

4. CONCLUSION

This work proposes to use visual-inertial tracking technology to automatically determine six-degrees of freedom for the detector position and orientation relative to the X-ray source focal spot. Furthermore, human pose estimation is used to help position the patient's anatomy in the imaging context. This capability is enabling for executing and combining X-ray views to affect a 3D tomography scan. The resulting system performance is analyzed by system simulation in the specific clinical context of 3D chest imaging for critically ill, bed-ridden patients. The visual-inertial tracking and anatomy positioning technology opens the possibility of new types of patient positioning assistance and new system capabilities, such as 3D tomographic acquisitions in the mobile environment.

REFERENCES

[1] Cant, J., Snoeckx, A., Behiels, G., Parizel, P. M., and Sijbers, J., "Can portable tomosynthesis improve the diagnostic value of bedside chest X-ray in the intensive care unit? A proof of concept study", European radiology experimental, 1(1), 20 (2017).

[2] Kelly, J., and Sukhatme, G. S., "Visual-Inertial Sensor Fusion: Localization, Mapping and Sensor-to-Sensor Self-calibration", IJRR, 30(1), 56-79 (2010).

[3] Little, K. J., Reiser, I., Liu, L., Kinsey, T., Sánchez, A. A., Haas, K., Mallory, F., Froman, C., and Lu, Z. F., "Unified Database for Rejected Image Analysis Across Multiple Vendors in Radiography", Journal of the American College of Radiology: JACR, 14(2), 208–216 (2017).

[4] https://physics.nist.gov/PhysRefData/XrayMassCoef/tab4.html

[5] Christ A., et al., "The Virtual Family - Development of Anatomical CAD Models of two Adults and two Children for Dosimetric Simulations", Physics in Medicine and Biology, 55, N23–N38 (2010).

[6] Zhao, Y., Tkaczyk E., and Pan, F., "Visual and inertial sensor fusion for mobile X-ray detector tracking", Proc. ACM SenSys, 643–644 (2020).

[7] Cao, Z., Simon, T., Wei, S. E., andSheikh, Y., "Realtime Multi-Person 2D Pose Estimation using Part Affinity Fields", Proc. CVPR (2017).

[8] Acuna, R., and Willert V., "Insights into the robustness of control point configurations for homography and planar pose estimation", arXiv preprint arXiv:1803.03025 (2018).

[9] Deller, T., et al., "Effect of acquisition parameters on image quality in digital tomosynthesis", Proc. SPIE, Medical Imaging (2007).